Journal of Environmental Radioactivity 166 (2017) 270–277

Contents lists available at ScienceDirect

Journal of Environmental Radioactivity

journal homepage: www.elsevier.com/locate/jenvrad

Estimation of the radon production rate in granite rocks and evaluation of the implications for geogenic radon potential maps: A case study in Central Portugal

A. Pereira [a, *], R. Lamas [b], M. Miranda [b], F. Domingos [b], L. Neves [a], N. Ferreira [c], L. Costa [a]

[a] CEMUC, Department of Earth Sciences, University of Coimbra, Coimbra, 3030-299, Portugal
[b] IMAR, Department of Earth Sciences, University of Coimbra, Coimbra, 3030-299, Portugal
[c] LNEG – National Laboratory of Energy and Geology, Rua do Ameal, 4466-901, S. Mamede de Infesta, Portugal

ARTICLE INFO

Article history:
Received 8 January 2016
Received in revised form
29 August 2016
Accepted 31 August 2016
Available online 13 September 2016

Keywords:
Radon
Emanation
Production rate
Geogenic maps
Portugal

Abstract

The goal of this study was to estimate radon gas production rate in granitic rocks and identify the factors responsible for the observed variability. For this purpose, 180 samples were collected from pre-Hercynian and Hercynian rocks in north and central Portugal and analysed for a) ^{226}Ra activity, b) radon (^{222}Rn) per unit mass activity, and c) radon gas emanation coefficient. On a subset of representative samples from the same rock types were also measured d) apparent porosity and e) apparent density. For each of these variables, the values ranged as follows: a) 15 to 587 Bq kg^{-1}, b) 2 to 73 Bq kg^{-1}, c) 0.01 to 0.80, d) 0.3 to 11.4 % and e) 2530 to 2850 kg m^{-3}. Radon production rate varied between 40 to 1386 Bq m^{-3} h^{-1}. The variability observed was associated with geologically late processes of low and high temperature which led to the alteration of the granitic rock with mobilization of U and increase in radon ^{222}Rn gas emanation. It is suggested that, when developing geogenic radon potential maps, data on uranium concentration in soils/altered rock should be used, rather than data obtained from unaltered rock.

1. Introduction

Risk maps are tools that can be used to minimize the impact of environmental factors, including radon gas. For this last case, geogenic radon potential maps have some advantages over those based only on indoor radon concentrations; this is because the former are based on criteria that are less influenced by climatic and anthropogenic variables.

Gruber et al. (2013) discusses in detail the criteria that are the basis of the development of radiogenic radon potential maps in Europe. One of those criteria is the use of uranium concentrations or ^{226}Ra activity in rock/soil, assuming a correlation between these elements and the production/exhalation of radon gas.

However, this correlation has been called into question in some studies (*e.g.*, Amaral et al., 2012; Sakoda et al., 2011), in part due to the high mobility of uranium in the surface or in the near subsurface induced from the alteration processes. Particularly when incorporated in primary sources more susceptible to alteration (as in the case of uraninite), uranium can easily migrate from the structure of the host material and precipitate in cracks, on the surface of the minerals or even be mobilized by circulating groundwater (Pereira et al., 2010) under appropriated pH conditions. In this case, precipitation may occur a large distance away from the primary source in fault materials or in rocks with a matrix of clay, which can originate mineral deposits of economic interest (Pereira and Neves, 2012). These processes may be intrinsic to the geologic unit, related with the mineralogical composition, or have a purely local character, inducing intra-unit variability in the latter.

One way to assess this variability involves using the emanation coefficient which can be obtained from the relationship between ^{226}Ra activity and radon exhaled. This data has been published for several rock types and soils (Girault et al., 2011; Hassan et al., 2011; Przylibski, 2000; Sakoda et al., 2010, 2011; Sroor et al., 2013; Stoulos et al., 2003). The existence of a significant variability in this parameter has been acknowledged by several authors. For example, in a review study, Sakoda et al. (2011) indicated values for granites that varied between 0.04 and 0.40. Girault et al. (2011) showed that part of this variability was associated with the degree of alteration

* Corresponding author.
E-mail address: apereira@dct.uc.pt (A. Pereira).

http://dx.doi.org/10.1016/j.jenvrad.2016.08.022
0265-931X/

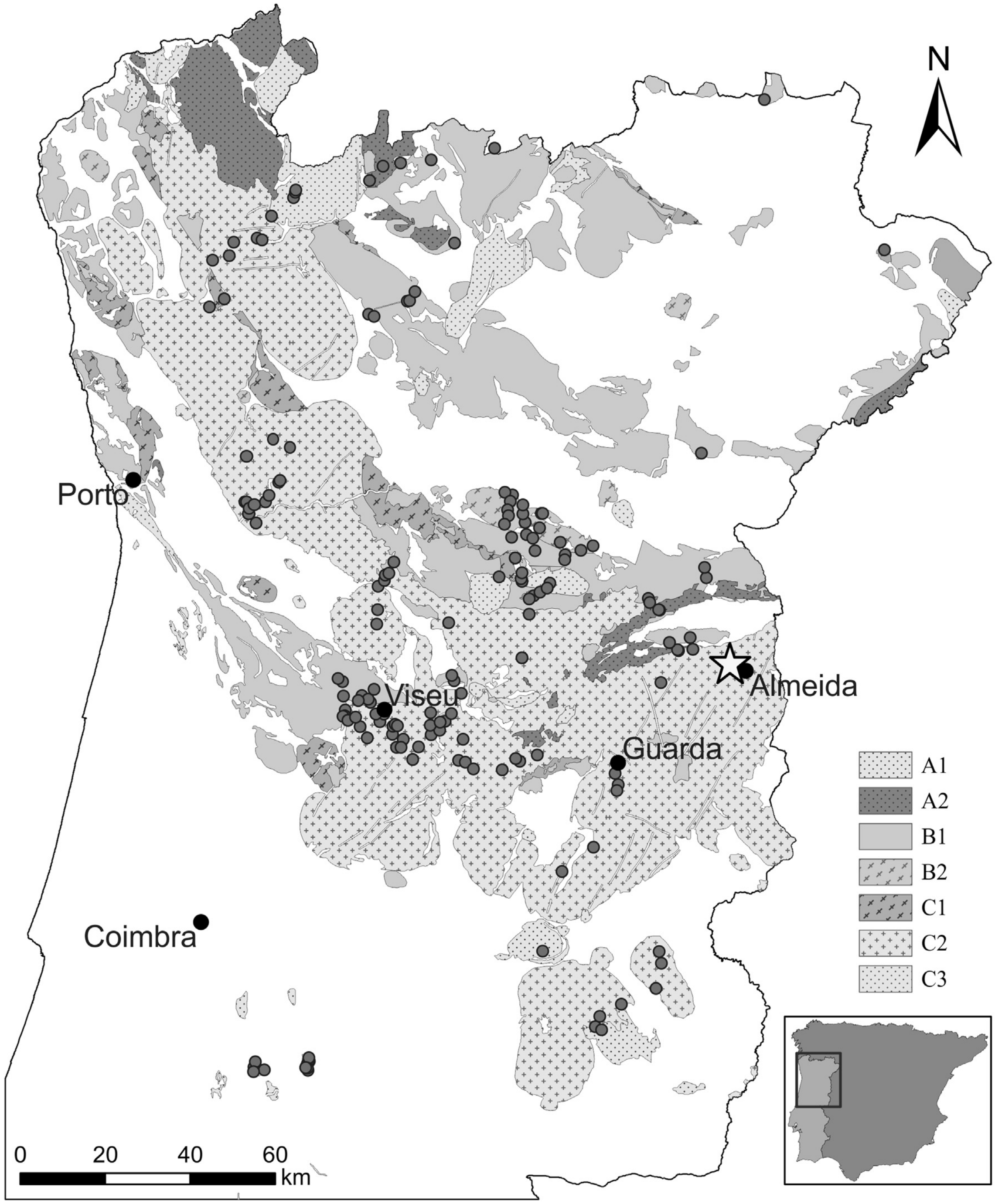

Fig. 1. Simplified geological map of the study area with the location of the samples set.

of the rock; this process enhanced the quantity of radon exhaled. Of course, porosity is an important control factor of the emanation factor, even though this parameter was not often measured (Banerjee et al., 2011).

Knowing the relationship between the ^{222}Rn and ^{226}Ra isotopes (expressed by the emanation coefficient) and the control factors is therefore an essential key in the assessment of the geogenic radon potential as well as in other problems involving the modeling of migration and transport of radon in geologic materials. However, it is also clear from the literature that there are few data available about the emanation coefficient, in particular about the factors, primary or secondary, that control its variability. .

The present work aimed to measure the activities of ^{226}Ra and ^{222}Rn and use these parameters to calculate the emanation coefficient in granitic rocks, which are the main lithology in the Northern and Central regions of Portugal. It also assessed the influence of control factors, particularly the effective porosity and density. Finally, this work assessed the quantity of radon exhaled from those geologic materials and for different degrees of alteration.

1.1. Geological setting

The granitic rocks that outcrop in large areas in Northern and Central Portugal are mostly of Hercynian age. They display high

Table 1
Descriptive statistics for ^{226}Ra and ^{222}Rn mass activities as well as the radon emanation coefficient (E) calculated for each granitic unit.

		^{226}Ra (Bq kg^{-1})	^{222}Rn (Bq kg^{-1})	E
A1 (n = 19)	μ ± σ	61 ± 37	18 ± 14	0.30 ± 0.18
	Med	57	13	0.29
	CV	0.60	0.76	0.59
	min − Max	15 to 160	4 to 57	0.08 to 0.68
A2 (n = 9)	μ ± σ	56 ± 20	13 ± 10	0.20 ± 0.11
	Med	56	9	0.17
	CV	0.35	0.78	0.57
	min − Max	16 to 79	3 to 33	0.07 to 0.45
B1 (n = 39)	μ ± σ	81 ± 28	24 ± 13	0.27 ± 0.13
	Med	78	21	0.28
	CV	0.35	0.54	0.46
	min − Max	34 to 172	4 to 64	0.07 to 0.71
B2 (n = 17)	μ ± σ	95 ± 35	32 ± 16	0.32 ± 0.10
	Med	85	29	0.32
	CV	0.36	0.49	0.30
	min − Max	45 to 178	11 to 73	0.14 to 0.48
C1 (n = 5)	μ ± σ	82 ± 16	15 ± 8	0.19 ± 0.12
	Med	71	11	0.10
	CV	0.20	0.55	0.65
	min − Max	65 to 102	8 to 30	0.09 to 0.40
C2 (n = 74)	μ ± σ	141 ± 96	20 ± 17	0.19 ± 0.18
	Med	117	15	0.12
	CV	0.68	0.84	0.95
	min − Max	22 to 587	2 to 70	0.01 to 0.80
C3 (n = 17)	μ ± σ	71 ± 30	22 ± 16	0.33 ± 0.19
	Med	74	18	0.29
	CV	0.42	0.71	0.59
	min − Max	27 to 140	3 to 59	0.05 to 0.75

Table 2
Descriptive statistics for apparent porosity and dry bulk density calculated for each granitic unit.

		Apparent porosity (%)	Apparent density (kg m^{-3})
A1 (n = 19)	μ ± σ	2.9 ± 1.4	2670 ± 19
	Med	2.5	2670
	CV	0.50	0.01
	min − Max	1.3 to 6.0	2640 to 2700
A2 (n = 3)	μ ± σ	2.1 ± 1.0	2680 ± 20
	Med	1.6	2670
	CV	0.47	0.01
	min − Max	1.3 to 3.5	2670 to 2710
B1 (n = 18)	μ ± σ	5.3 ± 2.1	2680 ± 55
	Med	5.3	2650
	CV	0.39	0.02
	min − Max	1.7 to 11.4	2620 to 2850
B2 (n = 5)	μ ± σ	5.8 ± 3.0	2700 ± 55
	Med	6.11	2670
	CV	0.52	0.02
	min − Max	2.4 to 10.5	2670 to 2810
C1 (n = 3)	μ ± σ	2.2 ± 1.1	2750 ± 59
	Med	1.9	2740
	CV	0.49	0.02
	min − Max	1.1 to 3.7	2680 to 2820
C2 (n = 34)	μ ± σ	1.9 ± 2.3	2660 ± 35
	Med	1.0	2660
	CV	1.2	0.01
	min − Max	0.3 to 9.2	2530 to 2760
C3 (n = 4)	μ ± σ	2.9 ± 1.5	2650 ± 29
	Med	2.4	2640
	CV	0.51	0.01
	min − Max	1.3 to 5.1	2610 to 2700

diversity in textural and mineralogical terms, and also in terms of their emplacement age (Fig. 1). Several classifications have been proposed to systematize the rocks of this type. At present, the one suggested in Ferreira et al. (1987) is used as a basis to the geological map of Portugal at a scale of 1: 1 000 000. This classification is based on the relationship between the emplacement age and the F_3 phase of the Hercynian orogeny.

Thus, the granitic rocks are organized as pre-Hercynian granites (A1), orthogneisses, sometimes with intermediate composition, earlier Hercynian migmatites and orthogneisses (A2), syn-tectonic two mica granites (B1), syn-to late-tectonic porphyritic granodiorites (C1), syn-to late-tectonic two mica granites (B2), late-to post-tectonic porphyritic biotite granites (C2) and post-tectonic biotite porphyritic granites (C3). Locally, some granites, mainly of the later porphyritic type, show post-emplacement mineralogical and textural transformation due to hydrothermal or metasomatic processes. Secondary uranium enrichment was also observed in faults that cross-cut this type of granite, being responsible for the emission of high gamma-ray fluxes. In some places the concentration was high enough to generate commercially exploited ore deposits in the past.

The granites intrude metasedimentary rocks ranging from Pre-Cambrian to Devonian in age and impose over them a thermal aureole of contact metamorphism of variable extension. Some of the metamorphosed metasedimentary rocks sometimes occur as enclaves in the granites.

2. Material and methods

A total of 180 representative samples were collected in outcrops of the different granitic units, having been taken into account the areal distribution of the outcrops (for the location of each sample see Fig. 1). The samples show different degrees of alteration and occur typically as fresh/unaltered to slightly altered.

A set of 21 samples was collected in the core of a deep borehole (with a well log of around 800 m) drilled in porphyritic biotite granites from the C2 group. The purpose of this borehole was to intersect a deep aquifer of thermal water and is located near Almeida town (Fig. 1). The sampling took into account findings from previous studies that indicated the occurrence of hydrothermal alteration confined to small areas of the core log (Lamas et al., 2015).

^{226}Ra activity was estimated by gamma-spectrometry techniques using an Ortec NaI(Tl) detector (3 × 3 inches) protected from background radiation with a lead shield, in the Laboratory of Natural Radioactivity of the University of Coimbra. The samples (with a weight of approximately 0.5 kg) were prepared at a grain size of less than 0.5 mm, placed in 0.2L Marinelli beakers (internal surface area of 0.0219 m^2), and left for one month to reach equilibrium in the ^{238}U chain before measurement. Counting was performed over 10 h, and the spectra were processed with Scintivison-32 software. The background was evaluated, using a Marinelli beaker filled with a radionuclide-free material (pure quartz) under the same analytical conditions, and subsequently subtracted from all samples. Calibration was achieved using standards from the International Atomic Energy Agency of known composition and activities; ^{226}Ra was estimated from the ^{214}Bi peak (1764.5 keV), assuming secular equilibrium. Uncertainty is strongly dependent on the radionuclide concentration and was estimated typically as 10% or less.

The same samples were used to determine radon exhalation. The samples were previously dried in an oven for 24 h at 40 °C and placed inside a 5 L radon-proof container made of stainless steel for 4 weeks. Radon activity was then measured with an AlphaGuard Pro monitor and its emanation coefficient (E) calculated from the following equation:

$$E = C_{eq}V/A_{Ra}W \tag{1}$$

where C_{eq} is the radon (^{222}Rn) concentration in the sealed container (Bq.m^{-3}) after the isotopic equilibrium is reached, V is

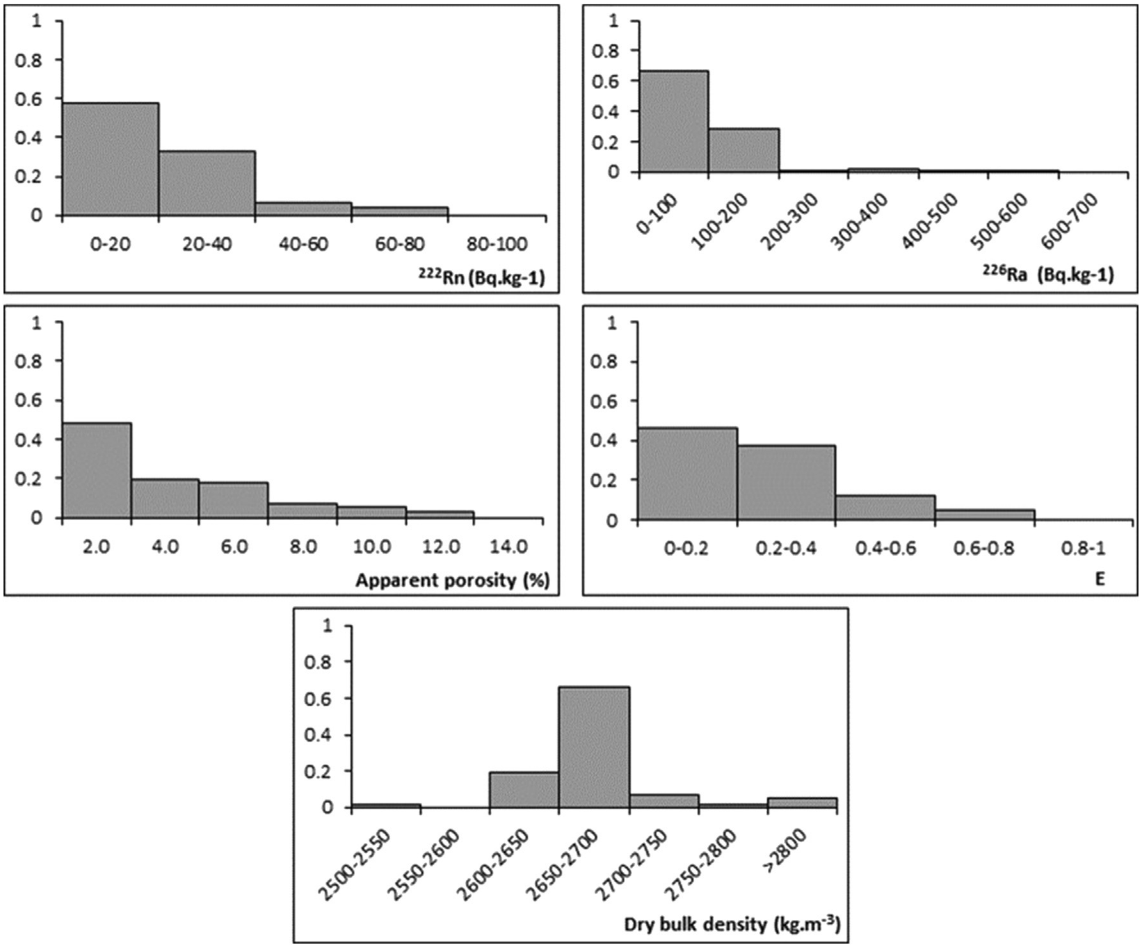

Fig. 2. Histograms obtained from the dataset relative to the different measured variables using a total of 180 samples for ^{226}Ra and ^{222}Rn mass activities and radon emanation coefficient measurements; for the remaining variables each histogram refers to a total of 86 samples.

the free volume of the container (m^{-3}), W is the weight of the sample (kg) and A_{Ra} is the ^{226}Ra mass activity (Bq kg^{-1}).

The apparent porosity (%) and apparent density (kg m^{-3}) were measured from samples that were first dried in an oven at a maximum temperature of 70 °C during 24 h and then weighed in order to obtain the dry weight (mass C). The specimens were then kept in a desiccator until they reached room temperature. Afterwards, a vacuum pump was used for 2 h to lower the pressure and remove the air present in the specimens' pores. The samples were then submerged by filling the container with water at a slow rate and keeping the pressure low during the assay. When all the samples were immersed, the vacuum pump was turned off in order to restore atmospheric pressure in the container. The samples remained immersed for 24 h, and, after that, suspended in water, weighed in order to determine the immersed weight (mass A) and then dried superficially and weighed once more to determine the saturated weight (mass B). Apparent porosity is given by (%) = (B-C)/(B-A) x 100, while apparent density is given by kg m^{-3} = B/(B-A) (EN, 1936:2006).

From the parameters above, radon production rate (P_{Rn}, in Bq m^{-3} h^{-1}) was also calculated using the following equation:

$$P_{Rn} = A_{Ra} E d \lambda \tag{2}$$

with d as the apparent density and λ the decay rate of ^{222}Rn.

3. Results

The data are summarized in Tables 1 and 2 as well as in the graphs of Fig. 2; they mainly include surface samples. As mentioned before, in the C2 group were also included core samples taken from the deep borehole of Almeida. In general, for all of the parameters, the values were distributed over a wide range. This trend was however different in the case of the apparent density. The distributions of values have a positive asymmetry and thus come close to a lognormal type distribution; most samples are clustered in the lower values. For apparent density the distribution shows more homogeneity, although it is clear that there is a positive asymmetry.

Regarding ^{226}Ra, more than 60% of the samples had an activity of less than 100 Bq kg^{-1}, ranging from 15 to 587 Bq kg^{-1}. A similar pattern was detected for ^{222}Rn activity and values ranged between 2 Bq kg^{-1} and 73 Bq kg^{-1}. Approximately 80% of the samples in which the emanation coefficient was estimated show values below 0.4 and within the range of 0.01–0.80. The measured porosity varied between 0.3 and 11%, while density varied between 2530 and 2850 kg m^{-3}. These fall within the ranges that have been reported for rocks of a similar nature (see Amaral et al., 2012; Cuccuru and Puccini, 2015; Sosna, 2012).

The distribution of ^{226}Ra activity in samples belonging to the different lithologic units under study (Fig. 3) indicated that the median is lower in older granites (pre-Hercynian or syn-F_3 Hercynian tectonic phase – A1 and A2) and higher in the porphyritic

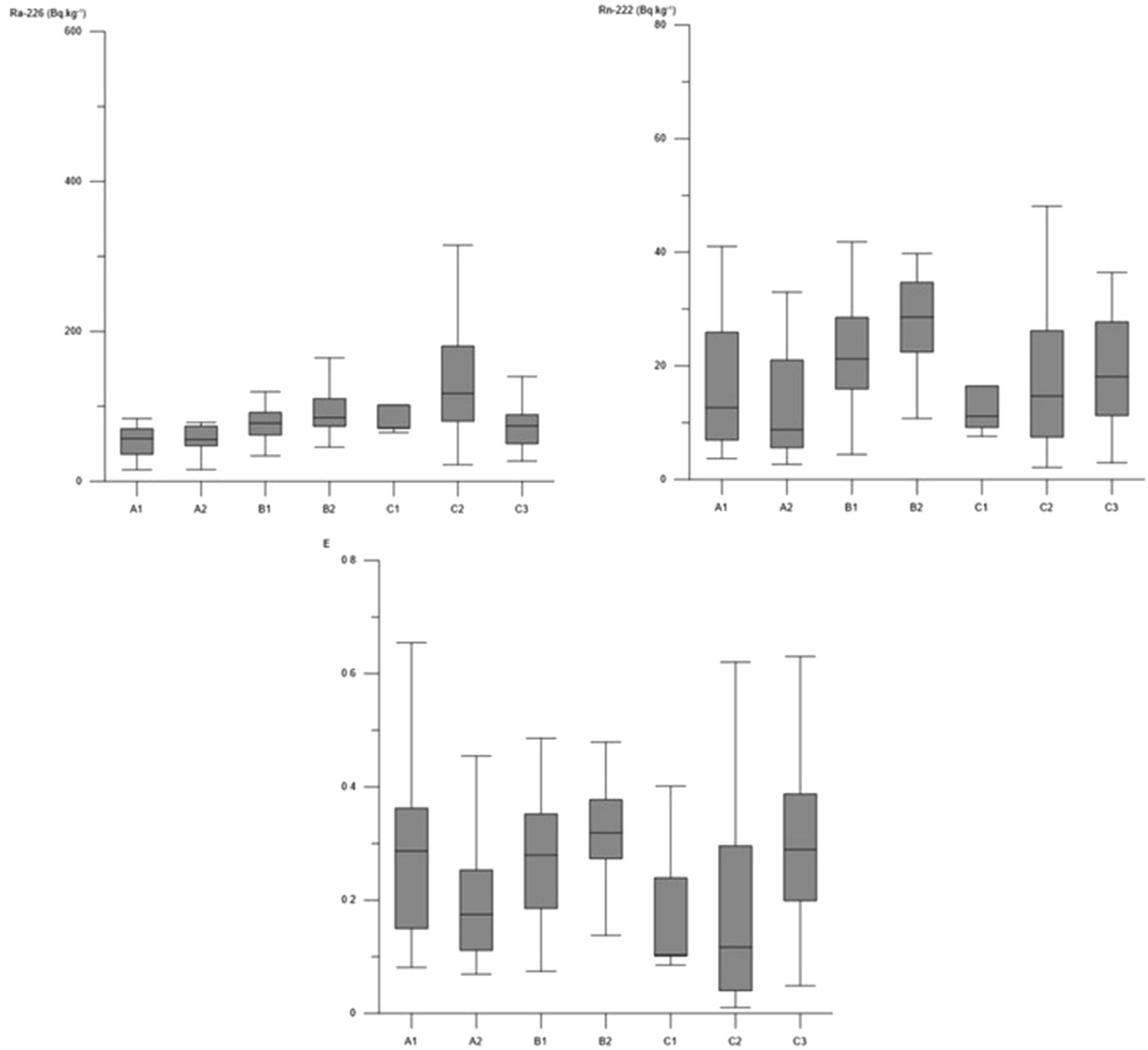

Fig. 3. Boxplot representation of basic statistical parameters estimated for ^{226}Ra and ^{222}Rn mass activities as well as the emanation coefficient (E).

Table 3
Correlation coefficient matrix with the different pairs of variables with those that are greater than the critical value for the level of significance of 0.01 (total of 86 samples).

	^{226}Ra (Bq kg^{-1})	^{222}Rn (Bq kg^{-1})	E	Porosity (%)	Density (kg m^{-3})
^{226}Ra (Bq kg^{-1})	1				
^{222}Rn (Bq kg^{-1})	*	1			
E	−0.69	0.85	1		
Porosity (%)	−0.56	0.68	0.80	1	
Density (kg m^{-3})	*	*	*	*	1

* Coefficient lower than the critical value for the same significance level.

biotite granites, late-to post-F$_3$ Hercynian tectonic phase (C2). The medians, used as an estimator of the central tendency of the distribution, ranged from 56 to 57 Bq kg^{-1} in the first case, while in the latter it assumes a value of 117 Bq kg^{-1}. The two-mica granites are in the intermediate range with a median activity of 78 Bq kg^{-1} (B1) and 85 Bq kg^{-1} (B2).

Exhaled radon had the same trend; older granites also had lower gas emanation capacity, with medians of 9 Bq kg^{-1} and 13 Bq kg^{-1}, respectively for groups A2 and A1 (Fig. 3). Exhaled radon activity measured in C1 samples (early granodiorites) falls within the same interval, with a median of 11 Bq kg^{-1} (Table 1). However, the situation changed for the remaining rocks: two-mica granites, B1 and B2, showed higher values, respectively 21 and 29 Bq kg^{-1}. In the samples from the porphyritic biotite granites, the C3 group also reversed the earlier trend, as it had the highest average of the set (22 Bq kg^{-1} and a median of 18 Bq kg^{-1}). In all of the cases, variability was significant, particularly with regards to potential radon gas exhalation, with variation coefficients higher or close to 50%. Variability was particularly important in the C2 group, wherein the coefficient of variation was the highest (84%).

As expected, the emanation coefficient followed a similar pattern of variation for exhaled radon activity (Fig. 3). However, the lowest medians corresponded to the porphyritic biotite granites, with values of 0.10 and 0.12, respectively for C1 and C2. The highest coefficients were calculated in samples of the two-mica granites (B1 − B2 and 0.28–0.32) as well as the C3 group from the porphyritic biotite granite.

Apparent porosity also had significant variation in samples of different lithologies (Table 2). Those with lower porosity belonged to groups A2, C1 and C2, and their median values are respectively 1.6%, 1.9% and 1.0%. The two-mica granites, on the other hand, clearly stood out from the studied set, with median porosities of 5.3% (B1) and 6.1% (B2).

For apparent density, the studied rocks were relatively homogeneous (Table 2). The median varied between 2640 and 2670 kg m^{-3}. Samples of group C1 had greater mass and more frequently had a value of 2740 kg m^{-3} (Table 2). This increase in density can be explained by the lithological specificity of this latter group, which consists of granodiorites instead of granites, the dominant lithology in other groups (Sosna, 2012).

4. Discussion

In order to investigate possible relationships between the different variables, the correlation coefficient matrix was first calculated (Table 3). Since the shape of the histograms for the different data populations (Fig. 2) was close to lognormal, it was decided to correlate the logarithms instead of the original data. Table 3 only shows coefficients considered significant for the probability of 99% (established from the theoretical distribution law as 0.30).

There were negative correlations between ^{226}Ra, emanation coefficient and porosity. The correlations were positive for the following pairs: ^{222}Rn – E, porosity – ^{222}Rn and porosity – E. To correctly interpret the correlations, the values were projected in binary graphics (e.g., Fig. 4). Fig. 4 illustrates the relationship between ^{226}Ra mass activity and emanation coefficient. It is clear from this figure that the negative correlation between the two variables was mainly induced by the high variability that affects the samples of the C2-type granites. As ^{226}Ra mass activity increased, there is a progressive reduction in the amount of exhaled radon, evaluated from the emanation coefficient.

It should be recalled that the C2 group included two different subsets, the one that was collected from surface rocks and the other that includes the deep borehole core samples. To study the possible differences between them, the samples from the C2 group were projected alone for the same parameters (Fig. 5). Based on this, it appears that the borehole samples (C2A) were in a cluster characterized by high values of ^{226}Ra activity, but also simultaneously by a decreased ability of radon gas emanation. In the C2A subset, it is further noted that the samples with higher emanation coefficients (E higher or close to 0.10) corresponded to those affected by hydrothermal alteration processes active after the crystallization of the magma by the end of the Hercynian orogeny, a situation which has already been described in detail by Lamas et al. (2015).

This finding raises the hypothesis that late alteration processes are responsible for the variability observed in the values the variables under study. They promote meteoric (at low temperature) and hydrothermal or metasomatic (at higher temperature) alteration. These processes generally favor an increase in the porous media matrix flow and in the mobilization of uranium, and concomitantly of the ^{226}Ra integrated in its decay chain. Therefore a positive correlation between the coefficient of emanation and the apparent porosity is observed (Table 3 and Fig. 6). The samples of two-mica granites (B) correspond to those with higher values of porosity and, simultaneously, radon gas emanation potential. These had a smaller range than those of the other group of granites and

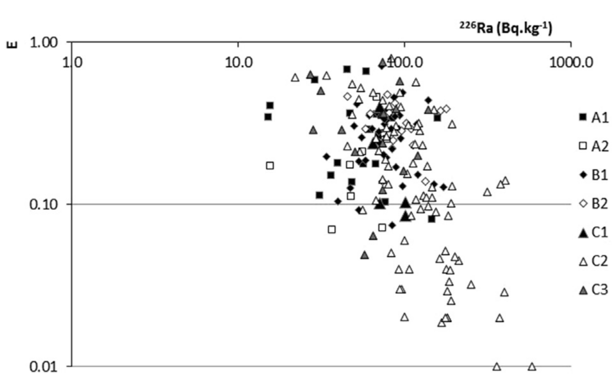

Fig. 4. Variation of ^{226}Ra mass activity with radon emanation coefficient (E) for the granite samples.

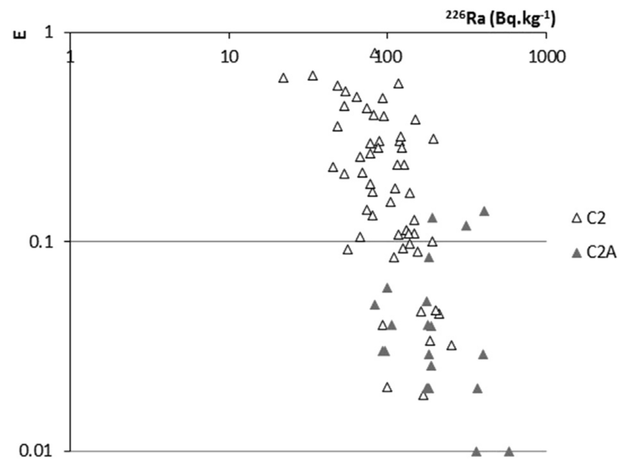

Fig. 5. Variation of ^{226}Ra mass activity with radon emanation coefficient (E) for samples of the porphyritic biotite granite (C2-type) collected in the surface and in borehole cores (C2A).

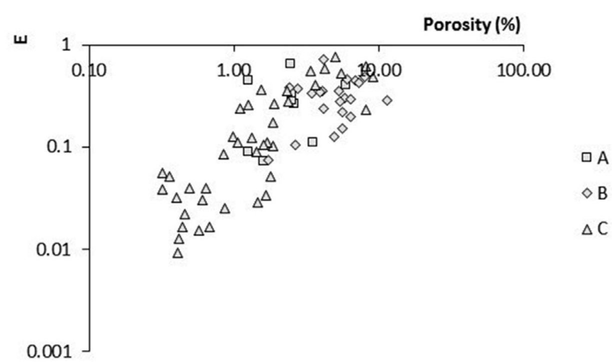

Fig. 6. Variation of the apparent porosity and radon emanation coefficient (E) for the granite samples (A – pre to earlier Hercynian, B – two-mica granites and C – porphyritic biotite granites).

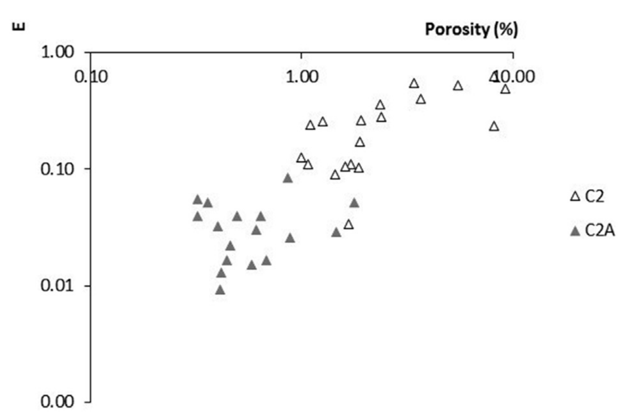

Fig. 7. Variation of the apparent porosity and radon emanation coefficient (E) for surface samples of the C2-type porphyritic biotite granite, excluding the dataset collected in the borehole (C2A).

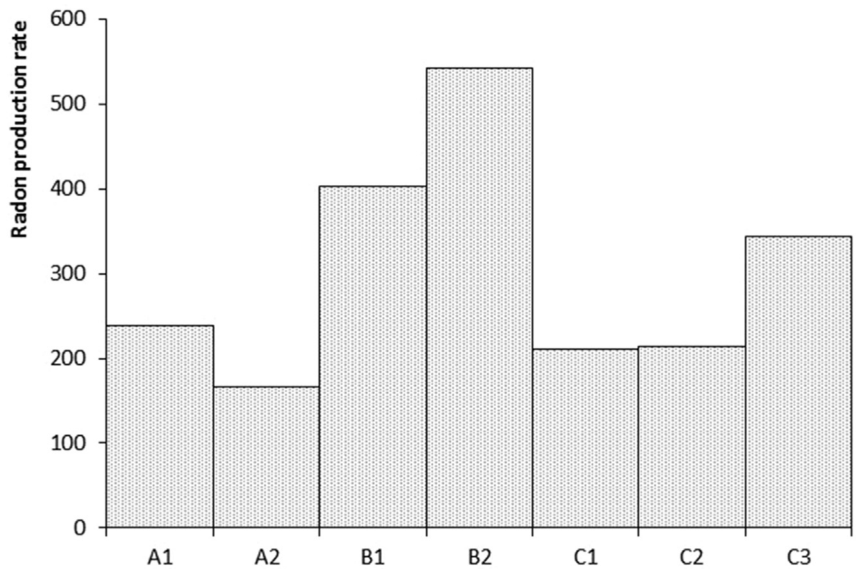

Fig. 8. Average radon production rate (median; in Bq m^{-3} h^{-1}) calculated for each granite unit.

Table 4
Radon production rate (in Bq m^{-3} h^{-1}) calculated for each granite unit.

A1 (n = 19)	μ ± σ	341 ± 267
	Med	239
	CV	0.78
	min − Max	70 to 1081
A2 (n = 9)	μ ± σ	240 ± 198
	Med	166
	CV	0.83
	min − Max	51 to 625
B1 (n = 39)	μ ± σ	445 ± 251
	Med	403
	CV	0.56
	min − Max	84 to 1212
B2 (n = 17)	μ ± σ	607 ± 304
	Med	542
	CV	0.50
	min − Max	203 to 1386
C1 (n = 5)	μ ± σ	283 ± 174
	Med	211
	CV	0.62
	min − Max	144 to 573
C2 (n = 74)	μ ± σ	301 ± 222
	Med	214
	CV	0.74
	min − Max	40 to 1331
C3 (n = 17)	μ ± σ	459 ± 346
	Med	343
	CV	0.75
	min − Max	56 to 1120

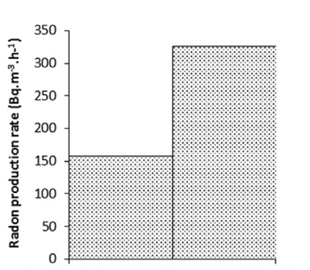

Fig. 9. Average radon production rate (median) calculated for surface samples of the C2-type granite (C2A surface) and cores of the deep borehole (C2A borehole).

also higher spatial expression (C). As in the case of ^{226}Ra − E relation, the cluster of the borehole data has the lowest potential for release of radon gas despite being the one that is most enriched in ^{226}Ra, as seen in Fig. 7.

On the basis of the estimated parameters for the different variables under study, and following equation (2), the potential of radon gas production for the different groups of granitic rocks outcropping in Northern and Central Portugal was calculated (Fig. 8 and Table 4). The two-mica granites are those with the most potential within the sample set, with a median of 402 Bq m^{-3} h^{-1} for B1, and 542 Bq m^{-3} h^{-1} for B2. For the same parameter, the porphyritic biotite granites showed values of 211 Bq m^{-3} h^{-1} (C1), 214 Bq m^{-3} h^{-1} (C2) and 343 Bq m^{-3} h^{-1} for C3. As expected, considering the previous results, the variability was also high in most cases, with variation coefficients always greater than 50%.

For group C2, however, it should be taken into account that these calculations also include samples of the deep borehole which, as was seen before, consistently showed lower values than the average ones obtained on the surface samples. To clarify the influence of this cluster in the average radon production rate of the C2 group, this group was subdivided into two sets: the surface samples and the deep borehole samples. The radon production rate median values for both sets are plotted in Fig. 9. This variable in the surface samples set is almost twice as high as the deep borehole samples. This finding shows the influence of the low temperature processes in the increase of the porosity and else the exhaled radon.

These conclusions were also reinforced by the results of another test involving a set of representative samples also of C2 granite but with a different degree of alteration and collected at the surface nearby the Almeida borehole-site. Table 5 and Fig. 10 show the results that were obtained including the estimated production of radon gas. Thereupon, the borehole samples were separated into two groups, one of unaltered samples and the other with evidence of hydrothermal alteration. Radon gas production potential was again much higher in the surface samples and it seems that the increase is proportional to the degree of alteration, probably due to the increase in porosity and emanation coefficient, which counterbalanced the effect of reduced ^{226}Ra activity.

So, the present study shows that the high temperature events increased the radon production in almost 3 times compared with

Table 5
Radon production rate (in Bq m^{-3} h^{-1}) calculated for the borehole samples (arithmetic mean values of each subset) and for 3 samples with different degree of alteration collected at the surface and nearby the borehole site.

		^{226}Ra (Bq kg^{-1})	^{222}Rn (Bq kg^{-1})	E	Porosity (%)	Density (kg m^{-3})	Radon production rate (Bq m^{-3} h^{-1})
Borehole samples	1 – Group I (n = 12)	210	4.6	0.03	0.51	2650	88
	2 – Group II (n = 9)	248	20	0.07	1.1	2650	382
Surface samples	3 – non-altered rock (n = 1)	112	21	0.18	2.1	2660	403.0
	4 – minimum degree of alteration (n = 1)	128	31	0.23	1.8	2640	598
	5 – medium degree of alteration (n = 1)	105	34	0.31	13.2	2640	653

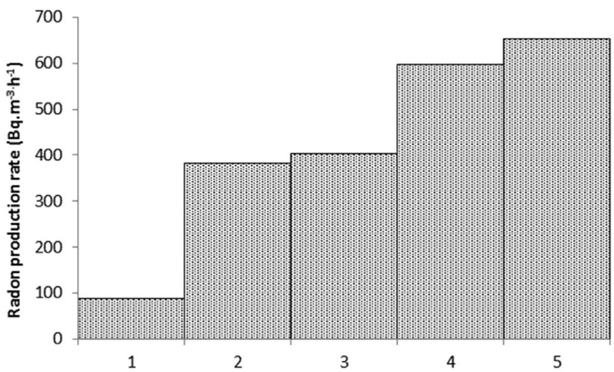

Fig. 10. Radon production rate calculated for samples of the borehole (1 – without evidences of hydrothermal alteration and 2 – with hydrothermal alteration) and surface samples of the same granite type but different degree of low temperature alteration (3 – fresh, 4 – minimum and 5 – medium altered). The values refer to the average per category of the samples.

the production of the group not affected by the same processes. The near surface weathering caused an increase close to one order of magnitude in the production of gas radon estimated from fresh to slightly altered rock samples.

5. Conclusions

The present work aimed to quantify a set of variables known to be involved in the control of radon gas production in Hercynian granitic rocks outcropping over a wide area of Northern and Central Portugal.

The data highlight the importance of porosity in radon emanation control from the studied rocks, which, in turn, depends on the existence of low and high temperature transformation processes that affect the granitic rocks after magmatic crystallization. These processes also contributed to remobilize uranium and, consequently, ^{226}Ra from the crystal structure.

Therefore, it is not always possible to establish a meaningful correlation between uranium (U) content and the geogenic radon concentrations, particularly if using data from unaltered rock or boreholes samples. The results obtained in this study indicated that the correlation is better when using uranium data collected in soils or altered rock and, therefore, should be preferred when developing radon geogenic potential maps. The same results can also help to explain the local variability, which is frequently reported in studies involving soil-gas radon concentration measurements.

References

Amaral, P.G.Q., Galembeck, T.M.B., Bonotto, D.M., Artur, A.C., 2012. Uranium distribution and radon exhalation from Brazilian dimension stones. Appl. Radiat. Isot. 70 (4), 808–817.

Banerjee, K.S., Basu, A., Guin, R., Sengupta, D., 2011. Radon (^{222}Rn) level variations on a regional scale from the Singhbhum Shear Zone, India: a comparative evaluation between influence of basement U-activity and porosity. Radiat. Phys. Chem. 80 (5), 614–619.

Cuccuru, S., Puccini, A., 2015. Petrographic, physical–mechanical and radiological characterisation of the rosa beta granite (Corsica-Sardinia batholith). In: Engineering Geology for Society and Territory, vol. 5. Springer International Publishing, pp. 233–236.

EN 1936, 2006. European Standard. Natural Stone Test Methods. Determination of Real Density and Apparent Density, and of Total and Open Porosity, p. 13.

Ferreira, N., Iglesias, M., Noronha, F., Pereira, E., Ribeiro, A., Ribeiro, M., 1987. Granitóides da zona Centro-Ibérica e seu enquadramento geodinâmico. In: F.Bea, A., Gonzalo, Carnicero, J., Plaza, M., Alsonso, M. (Eds.), Geologia de los granitoides y rocas associados del Macizo Hesperico, libro homenage a L.C. Figueirola. Editorial Rueda, Madrid, pp. 37–51.

Girault, F., Gajurel, A., Perrier, F., Upreti, B., Richon, P., 2011. Radon emanation of heterogeneous basin deposits in Kathmandu Valley. Nepal. J. Asian Earth Sci. 40 (2), 595–610.

Gruber, V., Bossew, P., Cort, M. De, Tollefsen, T., 2013. The European map of the geogenic radon potential. J. Radiol. Prot. 33, 51–60.

Hassan, N., Ishikawa, T., Hosoda, M., Iwaoka, K., Sorimachi, A., Sahoo, S., Janik, M., Kranrod, C., Yonehara, H., Fukushi, M., Tokonami, S., 2011. The effect of water content on the radon emanation coefficient for some building materials used in Japan. Radiat. Meas. 46 (2), 232–237.

Lamas, R., Miranda, M., Neves, L., Pereira, A., 2015. Radiogenic heat production from a deep borehole in the Beiras Granite (Almeida, Central Portugal). In: Energy for Sustainability, pp. 1–5.

Pereira, A.J.S.C., Neves, L.J.P.F., 2012. Estimation of the radiological background and dose assessment in areas with naturally occurring uranium geochemical anomalies—a case study in the Iberian Massif (Central Portugal). J. Environ. Radioact. 112, 96–107.

Pereira, A.J.S.C., Godinho, M.M., Neves, L.J.P.F., 2010. On the influence of faulting on small scale soil-gas radon variability – a case study in the Iberian uranium province. J. Environ. Radioact. 101, 875–882.

Przylibski, T., 2000. Estimating the radon emanation coefficient from crystalline rocks into groundwater. Appl. Radiat. Isot. 53 (3), 473–479.

Sakoda, A., Nishiyama, Y., Hanamoto, K., Ishimori, Y., Yamamoto, Y., Kataoka, T., Kawabe, A., Yamaoka, K., 2010. Differences of natural radioactivity and radon emanation fraction among constituent minerals of rock or soil. Appl. Radiat. Isot. 68 (6), 1180–1184.

Sakoda, A., Ishimori, Y., Yamaoka, K., 2011. A comprehensive review of radon emanation measurements for mineral, rock, soil, mill tailing and fly ash. Appl. Radiat. Isot. 69 (10), 1422–1435.

Sosna, K., 2012. Laboratory Determination of the Mechanical Properties of Granite Rocks. ARCADIS Geotechnika Inc, Prague, Czech Republic.

Sroor, A., Darwish, S., El-Bahi, S., Karim, M., 2013. Radiological hazards for marble and granite used at Shak El Thouban industrial zone in Egypt. J. Environ. Prot. 4, 41–48.

Stoulos, S., Manolopoulou, M., Papastefanou, C., 2003. Assessment of natural radiation exposure and radon exhalation from building materials in Greece. J. Environ. Radioact. 69 (3), 225–240.